ADVANCES IN MATERIALS SCIENCE, Vol. 20, No. 3(65), September 2020

DOI: 10.2478/adms-2020-0015

A. Gahtar[1,2], S. Benramache[1]*, C. Zaouche[1], A. Boukacham[3], A. Sayah[4]

[1] Material Sciences Department, Faculty of Science, University of Biskra, Biskra 07000, Algeria

[2] Biological department, University of El-Oued, El-Oued 39000, Algeria

[3] Unité de Physique des Dispositifs à Semiconduteurs, Faculté des Sciences de Tunis, Tunis El Manar University, Tunisia

[4] Department of Process Engineering, Faculty of Technology. Ferhat Abbas University Setif 1, 19000, Algeria

* benramache.said@gmail.com

EFFECT OF TEMPERATURE ON THE PROPERTIES OF NICKEL SULFIDE FILMS PERFORMED BY SPRAY PYROLYSIS TECHNIQUE

ABSTRACT

In this work, we have prepared new materials of the nickel sulfide thin films by using the spray pyrolysis technique for promising co-catalyst to improve the photocatalytic performance or superconductivity. The effect of deposition temperature (523, 573 and 623 K) on structural, optical and electrical properties was investigated. The XRD diffraction shows that the prepared nickel sulfide at 523, 573 and 623 K having an orthorhombic, hexagonal and hexagonal structure, which were Ni_3S_2, $Ni_{17}S_{18}$ and NiS_2, respectively. The minimum value of crystallite size (45,9 nm) was measured of deposited film at 573K. The thin films prepared at 523 and 573 K have an average transmittance is about 20 %. The prepared Ni_1S_2 thin film at T=623 K has the lowest calculated optical band gap and Urbach energy. The Ni_1S_2 thin film also has the best calculated of the refractive index and the extinction coefficient. The FTIR spectrums of the nickel sulfide have various bands such as Ni-S, C-H, O-H, N–H and C-S. The maximum electrical conductivity is $4{,}29x10^5$ $(\Omega.cm)^{-1}$ was obtained at 573K of the $Ni_{17}S_{18}$. The nickel sulfide thin films sprayed at 573K have good structural, optical and electrical properties.

Keywords: Nickel sulfide; thin films; spray pyrolysis; optical properties

INTRODUCTION

Metal chalcogenide thin films are particularly interesting for the fabrication of large-area photodiode arrays, solar selective coatings, solar cells, photoconductors, sensors etc [1]. Nickel sulfide belongs to the compound semiconductor materials. The nickel sulfide is a transition metal compound and an interesting material, showing metal-insulator transition by doping or as a function of temperature and pressure. Nickel sulfide compound shows antiferromagnetic semiconductor and paramagnetic properties in low and high-temperature phases, respectively, transition metal chalcogenides have attracted considerable attention during the past decade due to their unique physical and chemical properties, including their use as semiconducting, optical, magnetic, and catalytic materials [2]. Important transition

metal sulfides include, among others, cadmium sulfide [3,4], zinc sulfide [5], silver sulfide [6] as well as many different phases of copper sulfides [7-9]. Among those materials, nickel sulfide has been widely studied due to its various phases and stoichiometries, ranging from the nickel-rich compound Ni_3S_2, Ni_6S_5, Ni_7S_6, Ni_9S_8, NiS to sulfur-rich compounds like Ni_3S_4 and NiS_2 [10,11]. NiS is known to exist in two main phases, i.e. the hexagonal α-NiS, stable at elevated temperatures, and the rhombohedra β-NiS, which is stable at low temperatures [12].

Nickel sulfide has been recently used in many applications, such as materials for highly effective counter electrodes for solar cells [13-15] and seems to be an ideal material for supercapacitors [16-18] and cathodes for lithium batteries [19, 20].

It has been reported that cathode materials are currently the limiting factor preventing a wider application of lithium batteries in electric and hybrid vehicles and some of these shortages could be overcome by using metal sulfides as active cathode materials, and amongst them, NiS with a high theoretical capacity seems to be the most promising [21].

The mean object of this research is to study the synthesis of new nickel sulfide thin film by spray technique at different substrate temperatures. These materials can be used as a promising co-catalyst to improve the photocatalytic performance or superconductivity. In this research can be studied the physical properties such as the structural, morphological, optical and electrical characterizations. The effort of this study can be needed to optimize film properties in future investigations. Balayeva et al. [22] prepared nickel sulfide (NiS and Ni_3S_4) nanostructures at different sulfur sources like thiourea and sodium sulfide. However, Shinde et al. [23] investigated the sulfur Source-Inspired Self-Grown 3D Ni_xS_y Nanostructures and their electrochemical supercapacitors by hydrothermal method. Based on the past year, the nickel sulfide thin films can be deposited by various methods such as laser ablation (NiS) [24], successive ionic layer adsorption reaction (SILAR) technique [25], soft solution-processing (Ni_3S_2, NiS_2, and Ni_3S_4) [26], hydrothermal method (Ni_3S_2, NiS) [27] chemical vapor deposition (AACVD) method (NiS and $Ni_{17}S_{18}$) [28], and spray pyrolysis [29]. However, the deposition of nickel sulfide thin films by spray ultrasonic technique has yielded the best results, which is used in this work.

MATERIAL AND METHODS

Preparation of thin films

In this work, chloride nickel dehydrates 10^{-2}M ($NiCl_2$, $2H_2O$), and thiourea 2.10^{-2} M ($S=C(NH_2)_2$)) were used as precursors to prepare the nickel sulfide thin films. It was obtained from two solutions with different molarities; the mixture ([S]/[Ni]=2) was stirred for 3 hours at room temperature. The final solution was placed to the heater at 70 °C, in this setup, can be added drops of HCl solution as a stabilized (36%) to the mixture solution as a stabilized with heating. After this setup, the nickel sulfide solution becomes transparent and clear. Figure 1 shows the SPD experimental setup used here to deposit nickel sulfide thin films on glass substrates by spraying the nickel sulfide solution. The nickel sulfide thin films were performed on glass substrates (2x7 cm^2) by spray pyrolysis method with heating at different substrate temperatures (523, 573 and 623 K). The distance between the substrates and the spray gun nozzle was fixed at 3.5 cm. The solution and carrier gas flow rate was 4 ml/min, in all cases. We have used Nitrogen gas to avoid chemisorptions of oxygen to obtain the sulfide thin films without NiO films.

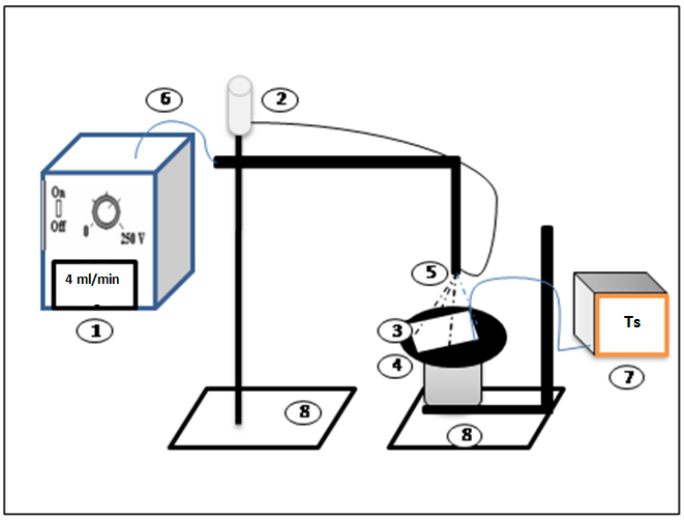

Fig. 1. Experimental layout used for SPD of nickel sulfide thin films: (1) power supply; (2) spray solution; (3) glass substrate; (4) four; (5) Electric gun; (6) switch between 1 and 2; (7) regulator of temperature; (8) supports for the heater and the gun

Characterization techniques

The structural properties of the nickel sulfide thin films were studied by X-ray diffraction (BRUKER-AXS type D8) equipment with X'Pert High Score under CuKα radiation λ=1.5406 Å with the scanning range of (2θ) was taken between 25 and 75 °. The surface morphologies of the nickel sulfide films were observed using a Q-Scope 250 atomic force microscope (Quesant Instrument Corporation) with contact mode scanning electron microscopy (SEM) coupled with microanalysis (EDX). The optical transmission and reflectance spectra were obtained using a UV-visible spectrophotometer (Shimadzu, Model 1800), the measurements have organized in the range of 300 – 1100 nm. The film thickness of the nickel sulfide (d) was measured by a well-known weight difference method taking into account the density of bulk nickel sulfide taken in this work (5.28 g / cm ^{3}). The investigation of nickel sulfide bond formation was obtained by Fourier transform infrared spectroscopy (Shimadzu IR-Infinity1), FT-IR measurements of nickel sulfide for all prepared samples were scanned in the range (400 - 4000 cm^{-1}), and film conductivity were measured by the four-point technique.

RESULTS AND DISCUSSION

X-ray diffraction analysis

Figure 2 shows the XRD diffraction patterns of nickel sulfide thin films deposited at different substrate temperatures by spray pyrolysis technique. The XRD diffraction shows that the prepared nickel sulfide at 523, 573 and 623 K having different phases and structures, which were Ni_3S_2 [30], $Ni_{17}S_{18}$ [31] and NiS_2 [32], respectively (see Table 1). As it can be seen the only diffraction peak was observed are (110), (015) and (010) plane at 2θ = 29,471 °, 29,351° and 29,309° of the sprayed nickel sulfide thin films at 523, 573 and 623 K, respectively (see Table 2). However, all thin films have high then one peak, which confirm that the preferred orientation was confined between these peaks; this observation indicates the polycrystalline in nature. The NiS_2 thin film prepared at 623 K has the two diffraction peaks intensities; this is attributed to the improvement of the crystalline structure of NiS_2 thin films.

On the other hand, we cannot observe other diffraction peaks related to the NiO phase. The main strain of the highest peak was calculated by the following relation [33]:

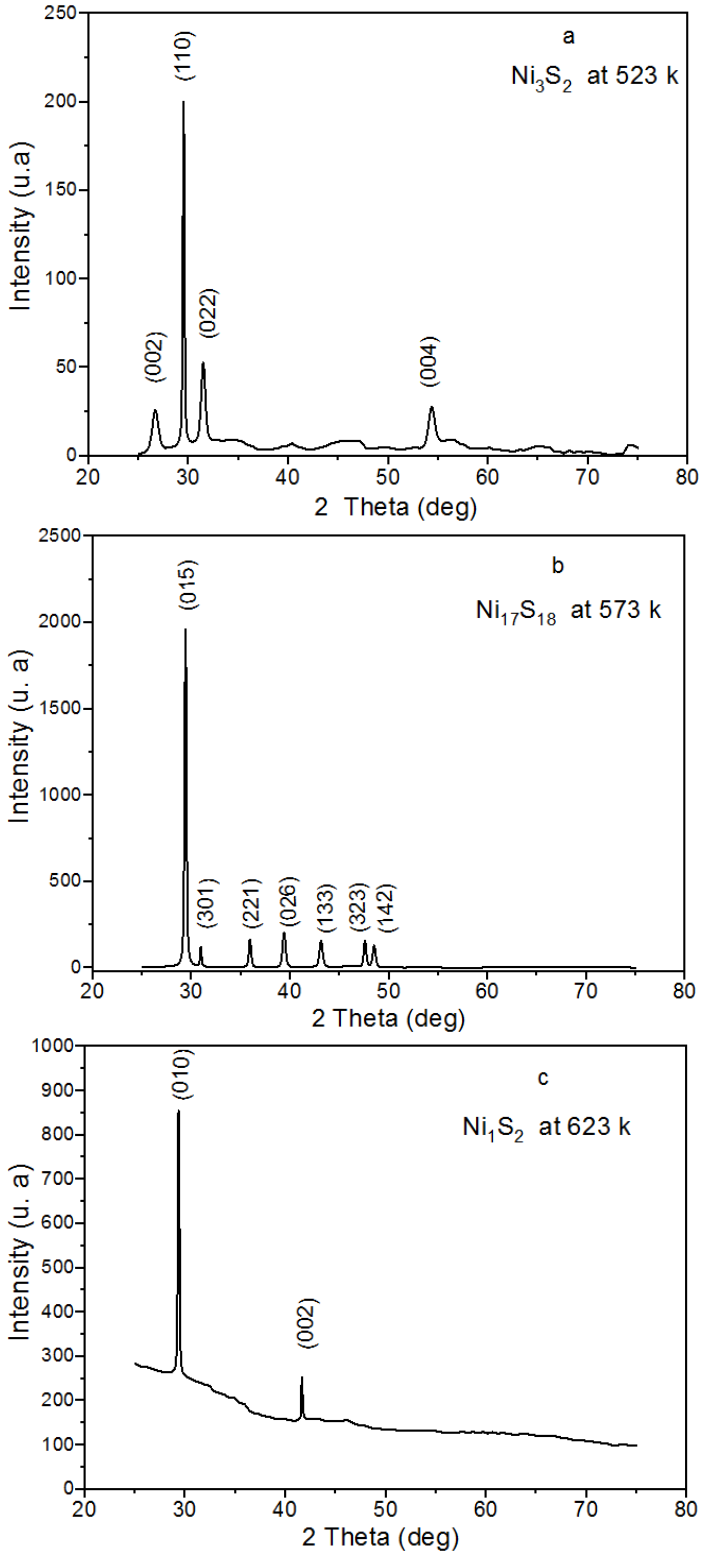

Fig. 2. XRD patterns of nickel sulfide thin films deposited on glass substrate at different substrate temperature: (a) 523 K, (b) 573 K, (c) 623 K

Table 1. *The phase structure of nickel sulphide thin films at different substrate temperatures*

Substrate temperature (K)	Name	Chemical formula	Crystal system	Space group	Reference
523	Nickel sulfide 3/2	Ni_3S_2	orthorhombic	Cm Cm 63	98-018-0767
573	Nickel sulfide 17/18	$Ni_{17}S_{18}$	hexagonal	P31 21 152	98-003-7164
623	Nickel sulfide 1/2	Ni_1S_2	hexagonal	P63/m mc 194	98-016-9577

Table 2. Values of Bragg angle 2θ , interplanar spacing d_{hkl}, full width at half maximum $\beta_{1/2}(rd)$, grain size *G.S*, micro strain ε and dislocation density δ for nickel sulfide thin films deposited on glass substrate at different substrate temperature: 523 K, 573 K, 623 K

Substrate temp (K)		2θ (deg.)	hkl	$\beta_{1/2}$ (rad)	G (nm)	ε x10^{-3} (%)	δ x10^{14} (cm^{-1})
Ni_3S_2	T=523	29.471	110	0,00288	49.8	2.936	4.0383
$Ni_{17}S_{18}$	T=573	29.351	015	0,00312	45.9	3.197	4.749
Ni_1S_2	T=623	29.309	010	0,00169	84.6	0.00173	1.400

$$\varepsilon = \frac{\beta}{4\tan\theta} \tag{1}$$

where ε is the mainstrain, β is the FWHM and θ is the half diffraction angle. On the other hand, the crystallite size values were estimated using Scherer equation [34]:

$$G = \frac{0.9\lambda}{\beta\cos\theta} \tag{2}$$

where G is the crystallite size, λ is the wavelength of X-ray (λ = 1.5406 A°). However, the dislocation density δ of nickel sulfide thin films was calculated from crystallite size by following relation [35]:

$$\delta = \frac{1}{G} \tag{3}$$

Table 2 shows the variation as a substrate temperature of the main strain, crystallite size and dislocation density of nickel sulfide thin films. As see, the lowest crystallite size was found for a deposited film at T=573 K corresponded to $Ni_{17}S_{18}$. As can be seen that the film deposited at 623 K (Ni_1S_2) has a minimum strain due to the equivalent in the number of atoms, also this film has a minimum dislocation density.

Structural morphology

To identify the morphology and chemical composition of nickel sulfide thin films, Figure 3 (a, b and c) present the structural morphology and the typical EDX spectrum of all deposited films at 523, 573 and 623 K, respectively. The porosity and the particle size of the NiS thin films were found as an overgrown cluster of the interconnected nano-flakes characterized via SEM analysis. The SEM image in Figure 3 shows a highly porous surface comprised of interconnected nano-flakes with sizes less than 100 nm together. It appears to us that the film surface was evenly covered without cracks and holes. Figure 3c shows an SEM image of deposited NiS thin film at 623 K exhibiting a nanosheet-like structure without cracks. This observation may facilitate the transmission of electrons and keep them with quite easily.

As see, the atomic percentage of Ni and S is 1.57 and 2.31%, respectively, for a deposited film at 523 K. The atomic percentage of Ni and S increased from 1.57 to 5.54% and 2.31 to 5.00%, respectively, with increasing deposition temperature from 523 to 573 K. Moreover,

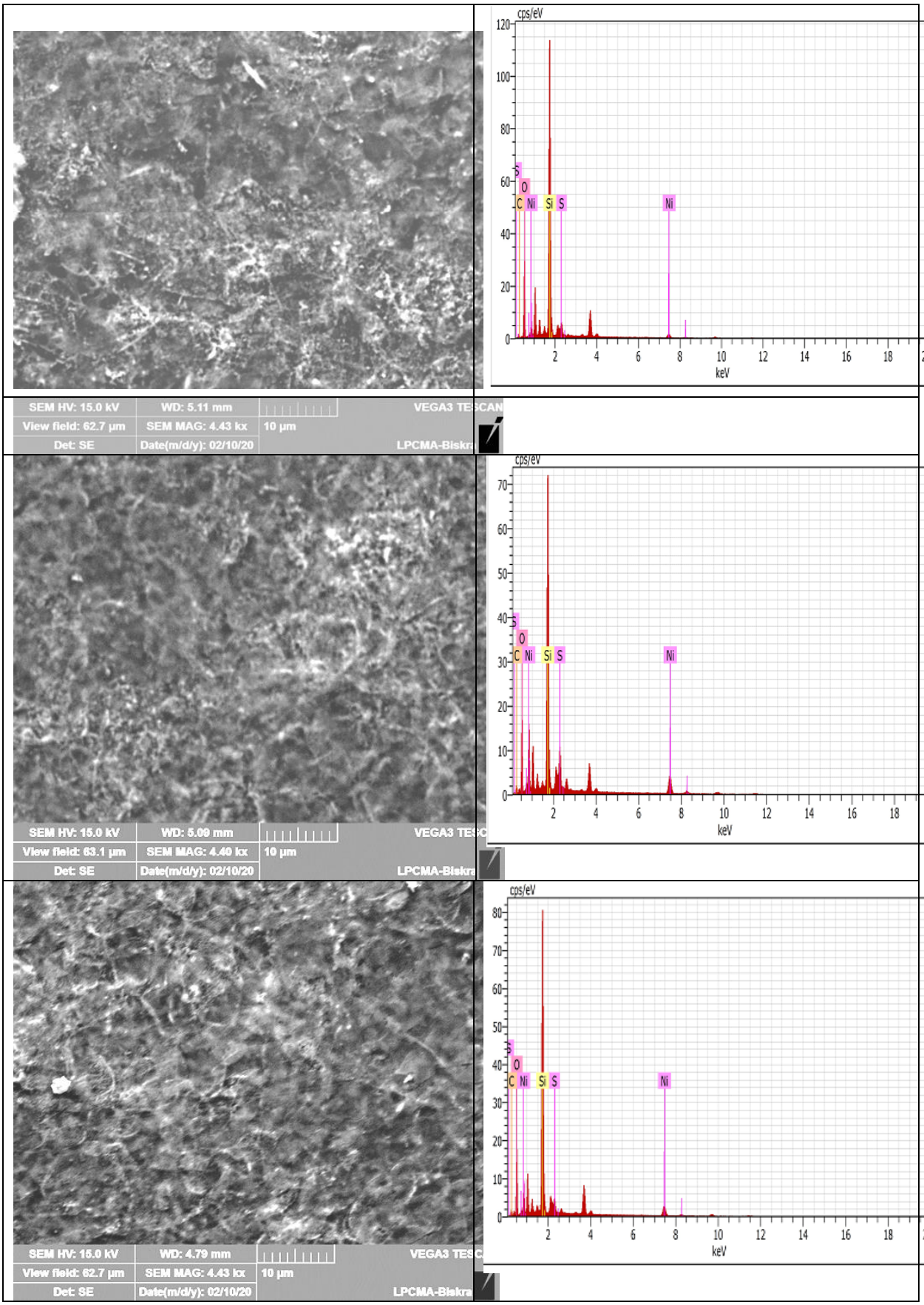

Fig. 3. SEM Image of nickel sulfide prepared at different substrate temperatures a) 523 K, b) 573 K, and c) 623 K

the percentage of Ni and S decreased when the substrate temperature increased to 623 K, which is 3.9 and 2.19%, respectively. The decrease of Ni and S at 623 K can be explained by the evaporation of S with deposition temperature, this is attributed to the corporation between Ni and S. However, the results EDX suggested that the nickel sulfide was successfully deposited on glass substrates. The other elements present in the spectrum such as oxygen (O) and silicon (Si) come from glass substrate (SiO_2) and precursors used in the deposition bath. From Figure 2, we cannot observe the NiO phase; this observation indicates that we cannot found a corporation between Ni and O.

Optical Properties

The optical spectra obtained to give the relative variation of the transmittance T (%) as a function of the wavelength λ (nm). In Figure 4, we have reported the variation of the optical reflectance (R) and transmittance (T) of nickel sulfide thin films deposited at different substrate temperatures 523 K, 573 K, 623 K. The reflectance of the nickel sulfide thin film increases with the wavelength and reaches 25% in the visible region, this phenomenon may be related to a metallic behavior. As can be seen that the transmittance of nickel sulfide thin films also increases, which is found in order to 20% in the visible region. The lowest value of transparency caroused by the color of nickel sulfide thin films. From the transmittance and reflectance spectrum of nickel sulfide thin films, the absorption coefficient of nickel sulfide can be calculated from the following relation [36]:

$$\alpha = \frac{1}{d} Ln\left(\frac{(1-R)^2}{T}\right) \tag{4}$$

where d is the film thickness, α is the absorption coefficient, T is the transmittance, R is the reflectance. The optical band gap energy E_g of nickel sulfide thin films was determined by the following relations [37]:

$$(\alpha h\upsilon)^{1/n} = C(h\upsilon - E_g) \tag{5}$$

where E_g is the optical band gap energy, C is a constant, is the photon energy ($h\nu = \frac{1240}{\lambda(nm)}(eV)$). The value of the exponent denotes the nature of the electronic transition, whether for direct allowed transitions n=1/2. However, Figure 5 shows the variation of the absorption coefficient α and the curve $(\alpha h\nu)^2 = f(h\nu)$ as a function of deposition temperature. However, the disorder or Urbach energy (E_u) also was determined by the expression follow [38]:

$$\alpha = \alpha_0 \exp\left(\frac{h\upsilon}{E_u}\right) \tag{6}$$

where α_0 is a constant $h\nu$ is the photon energy and E_u is the Urbach energy, the Urbach energy was used to characterizing the order of the defects. This energy confines the shape of the fundamental absorption edge in the exponential (Urbach) region and gives information on the structural disorder in the material. Figure 6 shows the variation of $Ln\alpha$ as a function $h\nu$

for estimated the Urbach energy (see Table 3). From Table 1, we have found that the minimum optical band gap and Urbach energy were obtained for sparing Ni_1S_2 at T=623K. This is confirmed that the temperature of 623K is suitable for preparing the Ni_1S_2 thin film with good optical gap energy and less disorder.

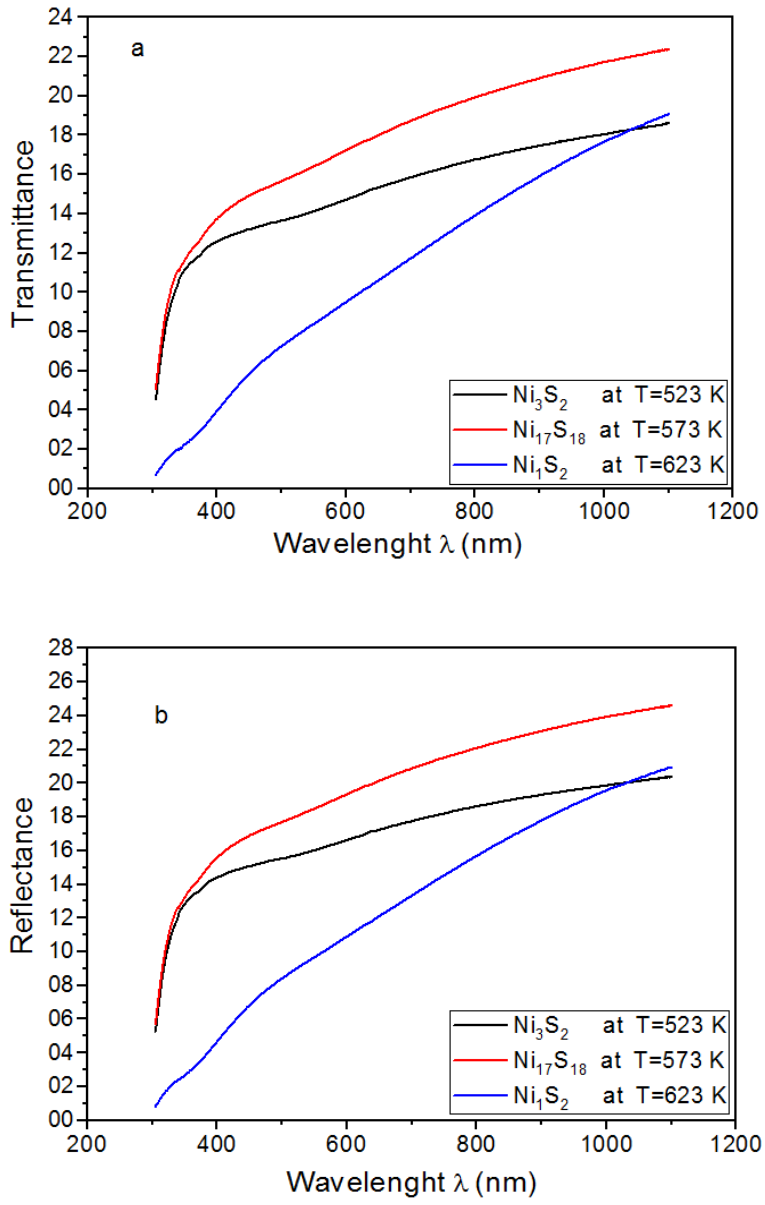

Fig. 4. Typical UV-Visible (a): Transmittance Spectrum and (b): reflectance of a thin layer of nickel sulfide prepared at different substrate temperatures

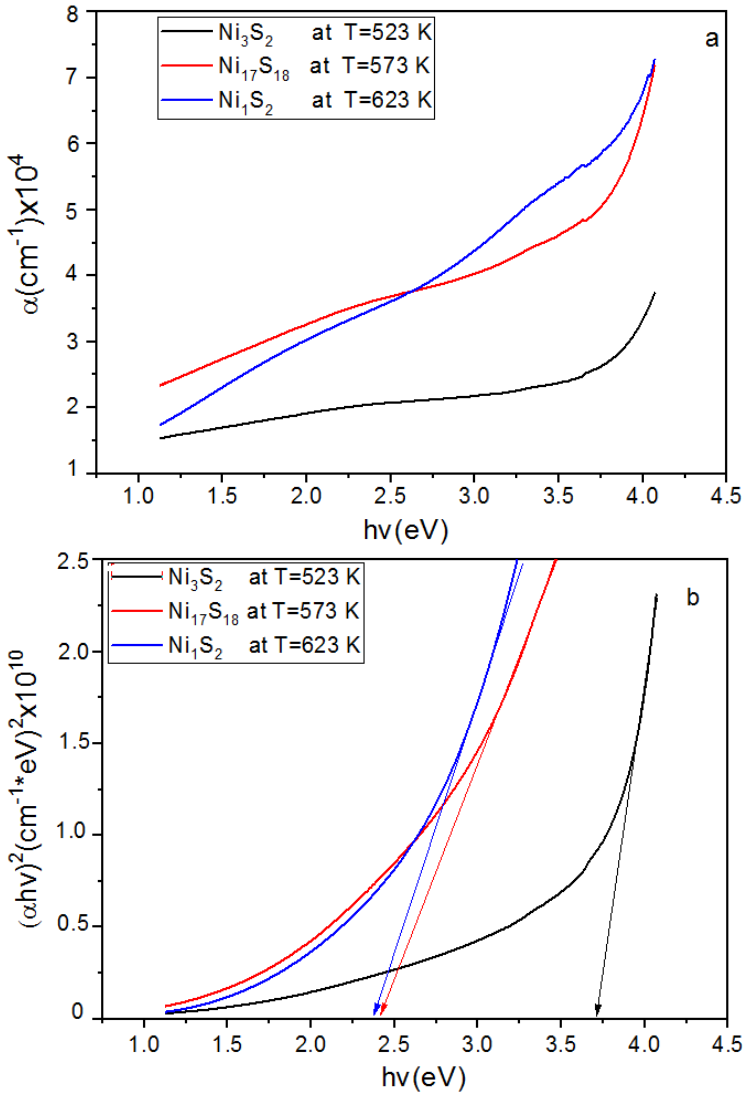

Fig. 5. The variation of the absorption coefficient α and the curve $(\alpha h\nu)^2 = f(h\nu)$ as a function of deposition temperature

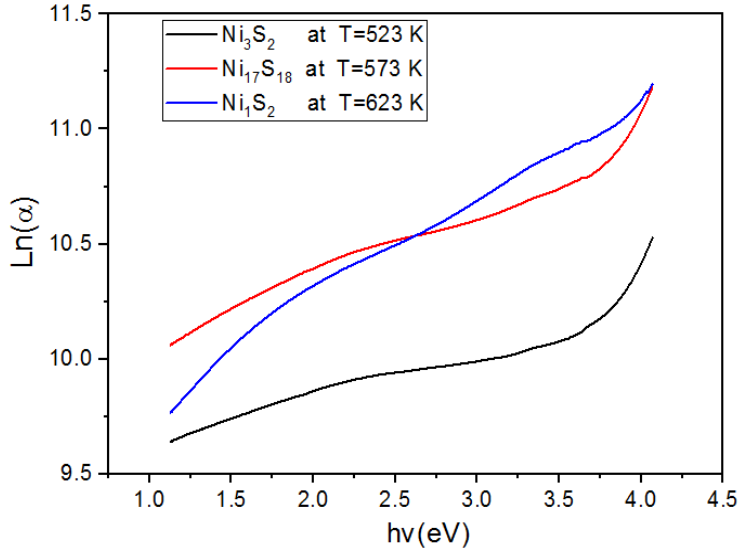

Fig. 6. The variation of $\ln(\alpha)$ vs $h\nu$ for nickel sulfide prepared at substrate temperatures 523 K, 573 K and 623 K

Table 3. *Optical properties of nickel sulphide thin films at different substrate temperatures*

Substrate temp (K)	E_g (eV)	E_u (meV)	σ_{opt} x10^{14} (S)
Ts=523	3.70	155.043	1.071
Ts=573	2.39	245.952	1.871
Ts=623	2.36	36.114	1.301

The extinction coefficient of nickel sulfide thin films with deposition temperature was calculated from Equation [39]:

$$k = \frac{\alpha\lambda}{4\pi} \tag{7}$$

where k is the extinction coefficient. However, the refractive index was calculated by the following relation [40]:

$$n = \frac{1+R}{1-R} + \sqrt{\frac{4R}{(1-R)^2} - k^2} \tag{8}$$

where n is the refractive index. The variation of the extinction coefficient and the refractive index are indicated in Figure 7.

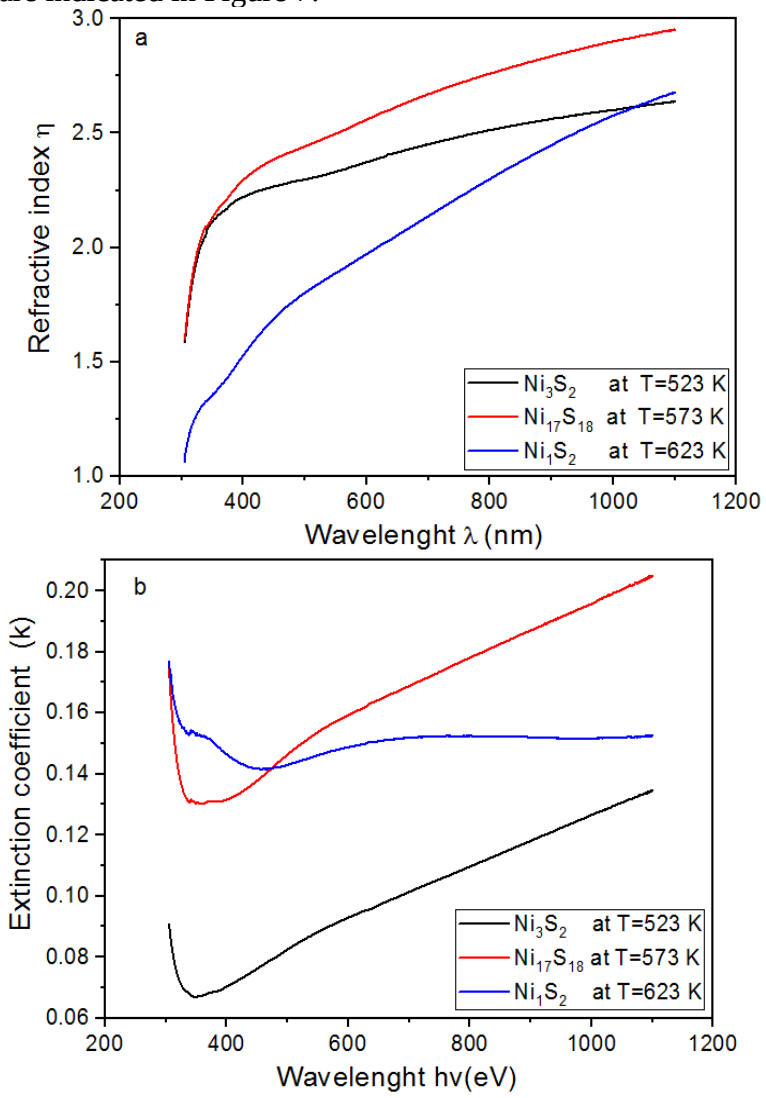

Fig. 7. The variation of refractive index n and extinction coefficient of sprayed nickel sulfide thin films deposited at substrate temperature 523 K, 573 K and 623 K

The optical conductivity also was determined with different deposition temperatures by the following equation [41]:

$$\sigma_{opt} = \frac{\alpha n c}{4\pi} \quad (9)$$

where c is the light velocity, n is the refractive index and σ_{opt} is the optical conductivity. The variation of the optical conductivity was presented in Figure 8. We observed that the optical conductivity increases by increasing the refractive index according to the equation above.

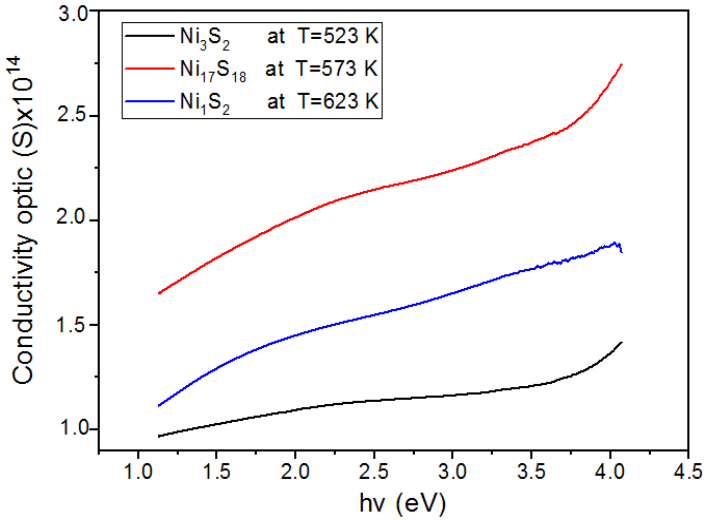

Fig. 8. The variation of optical conductivity σ_{opt} vs $h\nu$ for nickel sulfide prepared at different substrate temperatures 523 K, 573 K and 623 K

Figure 9 shows the variation of the dielectric constants ε_1 and ε_2 as a function of the wavelength. The values of ε_1 and ε_2 are deduced from n and k according to well-known relations [42,43]:

$$\begin{cases} \varepsilon_1 = n^2 - k^2 \\ \varepsilon_2 = 2nk \end{cases} \quad (10)$$

The FTIR spectrum of the nickel sulfide is shown in Figure 10, the peak at 601.79 cm^{-1} was attributed to the stretching vibration of Ni-S in the nickel sulfide phases [44]. The band at about 667.36 cm^{-1} and 875.68 cm^{-1} and 1037.7 cm^{-1} is attributed to the asymmetric stretching vibration of the C-S bond from the precursors [44]. The 1114.86 cm^{-1} band denotes the bending vibration of the sulfide functional group [45]. The bands observed at 2854.65 cm^{-1} and 2924.09 cm^{-1} were attributed to the C-H extension vibration of the precursor [46]. The broad peak at 3400 cm^{-1} corresponds to the N–H stretching of free amines. The presence of peaks around 1645 cm^{-1} corresponds to O-H stretching and bending vibrations [44-46]. Whereas band at around 601 cm^{-1} is resulting from the nickel sulfide lattice vibration [45]. It worth noting that absorption band at 601cm^{-1} appears in all spectra; this bond is evaluated using Hook's law giving by the following formula 18 [44]:

$$\bar{\nu} = \frac{1}{2\pi c}\sqrt{\frac{k}{\mu}} \quad (11)$$

where c is the light velocity, k is the bond force constant and μ is the reduced mass of nickel and sulfide. Thus the position of specific band absorption of nickel sulfide powders is determined with the basis of the 5.10^5 dynes/cm and the reduced mass $\mu=1/m_{Ni} + 1/m_S$ which leads to an absorption bond at 601 cm^{-1} closely to the observed one in all spectra of Figure 10.

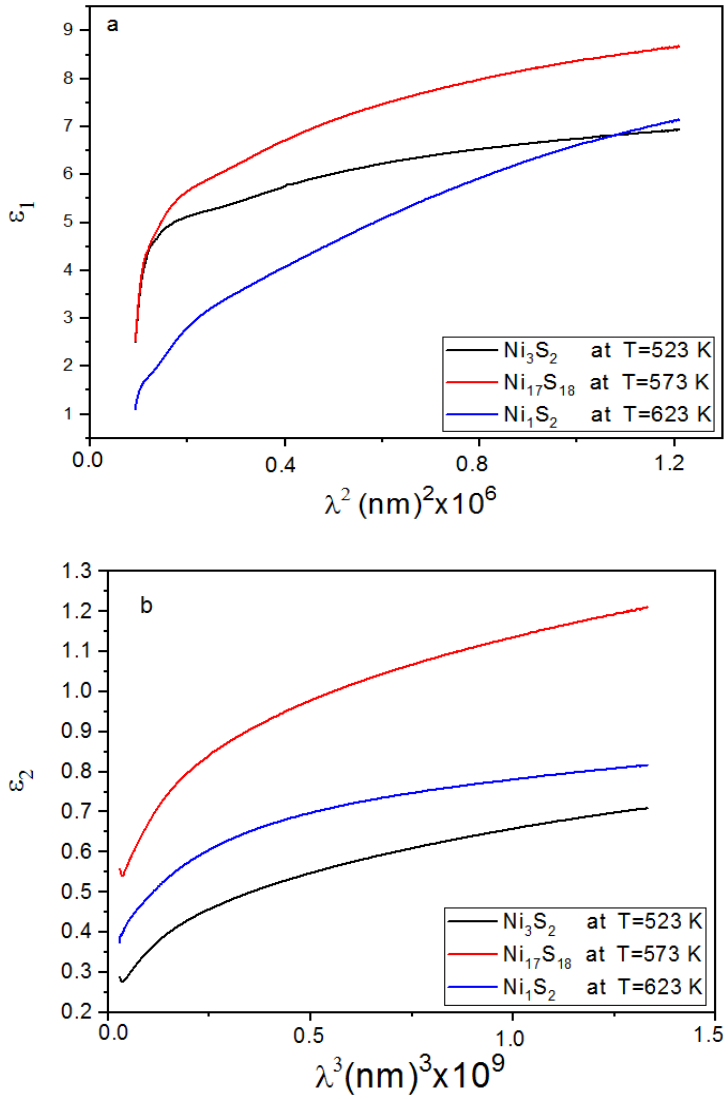

Fig. 9. The variation of ε_1 vs λ^2 and ε_2 vs λ^3 for nickel sulfide prepared at substrate temperatures 523 K, 573 K and 623 K

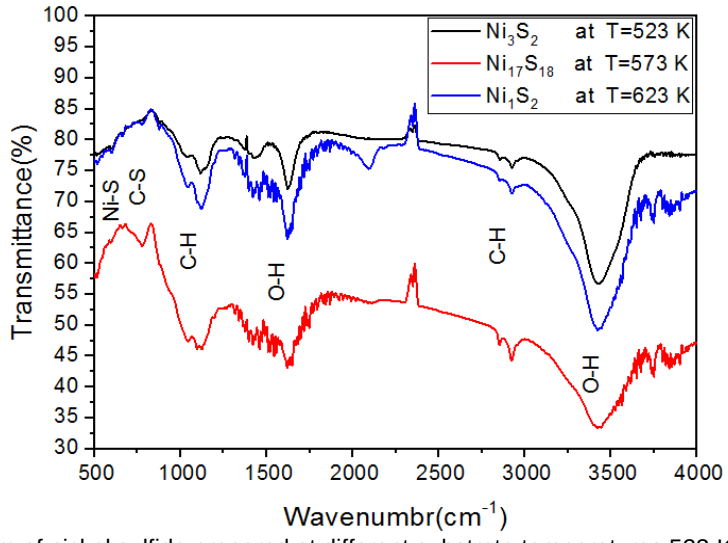

Fig. 10. FTIR spectrum of nickel sulfide prepared at different substrate temperatures 523 K, 573 K, and 623 K

Electrical properties

Table 4 presented the variation of the film thickness, electrical resistance, resistivity and conductivity of nickel sulfide thin films at different substrate temperatures. As shows that the electrical conductivity increased directly to sprayed thin film at 573 K then decreases with 623 K due to the high transmission and defects. The maximum electrical conductivity is $4{,}29x10^5$ $(\Omega.cm)^{-1}$, the reason to have a high electrical conductivity can be shown in the speed of the displacement of the electrons in the surface of a thin film with deposition temperature to the diffusion of S^{2-} donors and the substitutional sites of Ni^{2+}.

Table 4. *The film thickness and electrical properties of nickel sulphide thin films at different substrate temperatures*

Substrate temperature (K)	d(nm)	$R_{sh}(\Omega)$	Resistivity (Ω.cm)	Conductivity$(\Omega.cm)^{-1}$
Ts=523				
	798	0.201	1.60E-05	6.24E+04
Ts=573	390	0.0599	2.33E-06	4.29E+05
Ts=623	681	155	1.06E-02	9.47E+01

In Table 5 present the comparative results of our work with other researches; we have compared the structural, optical and electrical properties of the nickel sulfide thin films at several deposition temperatures. We observed that the nickel sulfide thin films sprayed at 573 K in this work have good crystallite size, lower optical band gap energy and good electrical properties,

Table 5. *The comparative study of the structural, optical and electrical properties of nickel sulfide thin films at different conditions*

Ts (K)	Phase	Deposition method	Film thickness (nm)	Crystallite size G (nm)	Optical energy E_g (eV)	Activation energy E_a (eV)	Electrical conductivity σ (Ω.cm)	Rf.
473	NiS	SESP		53	0.56		10^4	[1]
498-673	Ni_3S_2 6%Cu doped	PVD	-	90.8	2.1	-	-	[10]
	Ni_3S_2 10%Cu doped		-	90.8	1.89	-	-	
	Ni_3S_2			90.8	1.63	-	-	
300	NiS	SILAR	20-100	-	0.45	0.15	10	[25]
-	NiS	Spray pyrolysis	-	13-22	0.55	-	-	[38]
523	Ni_3S_2	Spray pyrolysis	798	49.8	3.70		$6.24.10^4$	This work
573	$Ni_{17}S_{18}$		390	45.9	2.39		$4.29.10^5$	
673	Ni_1S_2		681	84.5	2.36		$9.47.10^1$	

CONCLUSIONS

In summary, the nickel sulfide thin films were prepared by spray pyrolysis technique on a glass substrate at various deposition temperatures of 523, 573 and 623 K. The structural, optical and electrical properties of nickel sulfide thin films were investigated. The XRD diffraction shows that the prepared nickel sulfide at 523, 573 and 623 K having an orthorhombic, hexagonal and hexagonal structure, which were Ni_3S_2, $Ni_{17}S_{18}$ and NiS_2,

respectively. The minimum value of crystallite size (45,9 nm) was measured of deposited film at 573K. The thin films prepared at 523 and 573 K have a good transmittance is about 20 %. The Ni_1S_2 thin film has a minimum optical band gap and Urbach energy was obtained at T=623 K. The nickel sulfide thin films have a good refractive index and extinction coefficient. The FTIR spectrums of the nickel sulfide have various bands such as Ni-S, C-H, O-H, N–H and C-S. The maximum electrical conductivity is $4{,}29x10^5$ $(\Omega.cm)^{-1}$ was obtained at 573K of the $Ni_{17}S_{18}$. The nickel sulfide thin films sprayed at 573 K have good structural, optical and electrical properties, this thin film can be used a promising co-catalyst to improve the photocatalytic performance or superconductivity.

REFERENCES

1. Kumar V., Sharma D.K., Sharma K., Dwivedi D.K., Investigation on physical properties of polycrystalline nickel sulphide films grown by simple & economical screen-printing method, Optik 156 (2018) 43–48.
2. Kershaw S.V., Susha A.S., Rogach A.L., Narrow bandgap colloidal metal chalcogenide quantum dots: synthetic methods, heterostructures, assemblies, electronic and infrared optical properties, Chem. Soc. Rev. 42 (2013) 3033–3087.
3. Chand P., R. Ghosh, Sukriti, Investigation of structural, morphological and optical properties of Zn doped CdS nanostructures synthesized via co-precipitation method, Optik 161 (2018) 44–53.
4. He J., Mei Y., Zheng W.C., United calculation of the optical and EPR spectral data for $Co2^+$-doped CdS crystal, Optik 194 (2019) 163087.
5. Behboudnia M., Majlesara M.H., Khanbabaee B., Preparation of ZnS nanorods by ultrasonic waves, Mater. Sci. Eng. B 122 (2005) 160–163.
6. Kristl M., Gyergyek S., Kristl J., Synthesis and characterization of nanosized silver chalcogenides under ultrasonic irradiation, Mater. Express 5 (2015) 359–366.
7. Erken O., Gunes M., Kirmizigul F., Gumus C., Investigation of properties the copper sulfide thin films prepared from different copper salts, Optik 168 (2018) 884–891.
8. Xu H., Wang W., Zhu W., Sonochemical synthesis of crystalline CuS nanoplates via an in situ template route, Mater. lett. 60 (2006) 2203–2206
9. Kristl M., Hojnik N., Gyergyek S., M. Drofenik, Sonochemical preparation of copper sulfides with different phases in aqueous solutions, Mater. Res. Bull. 48 (2013) 1184–1188.
10. Majid S., Ahmad K.S., Analysis of dopant concentration effect on optical and morphological properties of PVD coated Cu-doped Ni3S2 thin films, Optik 187 (2019) 152–163.
11. Yin P.F., Sun L.L., Zhou C., Sun Y.H., Han X.Y., Deng C.R., Characterization and magnetic property of 3D flower-like nickel sulphide nanocrystals through decomposing bis(thiourea) nickel(II) chloride crystals, Bull. Mater. Sci. 38 (2015) 95–99.
12. Surendran S., Sankar K.V., Berchmans L.J., Selvan R.K., Polyol synthesis of α-NiS particles and its physic-chemical properties, Mater. Sci. Semicon. Proc. 33 (2015) 16–23.
13. Kim H.J., Yeo T.B., Kim S.K., Rao S.S., Savariraj A.D., Prabakar K., Gopi C.V. V.M., Optimal-Temperature-Based Highly Efficient NiS Counter Electrode for Quantum-Dot-Sensitized Solar Cells, Eur. J. Inorg. Chem. (2014) 4281–4286.
14. Kim H.J., Kim S.W., Gopi C.V.V.M., Kim S.K., Rao S.S., Jeong M.S., Improved performance of quantum dot-sensitized solar cells adopting a highly efficient cobalt sulfide/nickel sulfide composite thin film counter electrode, J. Power Sources 268 (2014) 163–170.

15. Gopi C.V.V.M., Rao S.S., Kim S.-K., Punnoose D., Kim H.-J., Highly effective nickel sulfide counter electrode catalyst prepared by optimal hydrothermal treatment for quantum dot-sensitized solar cells, J. Power Sources 275 (2015) 547–556.

16. Sun C.C., Ma M.Z., Yang J., Zhang Y.F., Chen P., Huang W., Dong X.C., Phase-controlled synthesis of alpha-NiS nanoparticles confined in carbon nanorods for high performance supercapacitors, Sci. rep. 4 (2014) 7054.

17. Chen H.C., Jiang J.J., Zhao Y.D., Zhang L., Guo D.Q., Xia D.D., One-pot synthesis of porous nickel cobalt sulphides: tuning the composition for superior pseudocapacitance, J. Mate. Chem. A 3 (2015) 428–437.

18. Yu L., Yang B., Liu Q., Liu J., Wang X., Song D., Wang J., Jing X., Interconnected NiS nanosheets supported by nickel foam: Soaking fabrication and supercapacitors application, J. Electroanal. Chem. 739 (2015) 156–163.

19. Wang Y., Zhu Q.S., Tao L., Su X.W., Controlled synthesis of NiS hierarchical hollow microspheres with different building blocks and their application in lithium batteries, J. Mater. Chem. 21 (2011) 9248–9254.

20. Tao H.C., Yang X.L., Zhang L.L., Ni B.B., One step synthesis of nickel sulfide/N-doped graphene composite as anode material for lithium ion batteries, J. Electroanal. Chem. 739 (2015) 36–42.

21. Zhang Z.J., Zhao H.L., Zeng Z.P., Gao C.H., Wang J., Xia Q., Hierarchical architecture NiS@SiO_2 nanoparticles enveloped in grapheme sheets as anode material for lithium ion batteries, Electrochim. Acta 155 (2014) 85–92.

22. Balayeva O.O., Azizov A.A., Muradov M.B., Maharramov A.M., Eyvazova G.M., Alosmanov R.M., Mamiyev Z.Q., Aghamaliyev Z.A., β-NiS and Ni_3S_4 nanostructures: Fabrication and characterization, Mater. Res. Bull. 75 (2016) 155-161.

23. Shinde N.M., Xia Q.X., Shinde P.V., Yun J.M., Mane R.S., Kim K.H., Sulphur Source-Inspired Self-Grown 3D NixSy Nanostructures and Their Electrochemical Supercapacitors, ACS Appl. Mater. Inter. 11 (2019) 4551-4559.

24. Lee H., Kanai M., Kawai T., Kawai S., Growth of Oriented NiS Films on Si(111) and $Al_2O_3(O_{12})$ Substrate by Pulsed Laser Ablation, Jpn. J. Appl. Phys. 32 (1993) 2100.

25. Sartale S.D., Lokhande C.D., Preparation and characterization of nickel sulphide thin films using successive ionic layer adsorption and reaction (SILAR) method, Mater. Chem. Phys. 72 (2001) 101-104.

26. Yu S.H., Yoshimura M., Fabrication of Powders and Thin Films of Various Nickel Sulfides by Soft Solution-Processing Routes, Adv. Funct. Mater. 12 (2002) 277-285.

27. Zhang L., Yu J.C., Mo M., Wu L., Li Q., Kwong K.W., General Solution-Phase Approach to Oriented Nanostructured Films of Metal Chalcogenides on Metal Foils: The Case of Nickel Sulfide, J. Am. Chem. Soc. 126 (2004) 8116–8117.

28. Akhtar M., Revaprasadu N., Malik M.A., Raftery J., Deposition of phase pure nickel sulfide thin films from bis(O-alkylxanthato)–nickel(II) complexes by the aerosolassisted chemical vapour deposition (AACVD) method, Mater. Sci. Semicon. Proc. 30 (2015) 368–375.

29. Mahadik A.S., Khalate S.A., Kate R.S., Deokate R.J., Chemical Spray Deposited Nickel Sulphide Thin Films for Supercapacitor applications, I. Res. J. Sci. Eng. Special Issue A1 (2017) 195–198.

30. Cheng Z., Abernathy H., Liu M., Raman Spectroscopy of Nickel Sulfide Ni_3S_2, J. Phys. Chem. C 111 (2007) 17997-18000.

31. Saeed S., Rashid N., Growth and characterization of semiconducting nickel sulfide nanocrystals from air-stable single-source metal organic precursors, Cogent Chem. 1 (2015) 1030195.

32. Chen F., Yang H., Wang X., Yu H., Facile synthesis and enhanced photocatalytic H2-evolution performance of NiS2-modified g-C3N4 photocatalysts, Chinese J. Catal. 38 (2017) 296–304.
33. Benramache S., Aoun Y., Lakel S., Benhaoua B., Torchi C., The calculate of optical gap energy and urbach energy of Ni1−xCoxO thin films, Sādhanā 44 (2018) 26.
34. Klug H.P., Alexander L.E., X-ray diffraction procedures: for polycrystalline and amorphous materials, X-Ray Diffraction Procedures: For Polycrystalline and Amorphous Materials, 2nd Edition, by Harold P. Klug, Leroy E. Alexander, pp. 992. ISBN 0-471-49369-4. Wiley-VCH, May 1974, p. 992, 1974.
35. Ho T.A., Bae C.k., Nam H., Kim E., Lee S.Y., Park J.H., Shin H., Metallic Ni3S2 Films Grown by Atomic Layer Deposition as an Efficient and Stable Electrocatalyst for Overall Water Splitting, ACS Appl. Mater. Inter. 16 (2018) 12807–12815.
36. Dias da Silva J., Campomanes R., Leite D., Orapunt F., O'Leary S.K., Relationship between the optical gap and the optical-absorption tail breadth in amorphous GaAs, J. appl. Phys. 96 (2004) 7052-7059.
37. Tauc J., Menth A., States in the gap, J. non-cryst. Solids 8 (1972) 569-585.
38. Urbach F., The long-wavelength edge of photographic sensitivity and of the electronic absorption of solids, Phys. Rev. 92 (1953) 1324.
39. Benramache S., Aouassa M., Preparation and Characterization of p–Type Semiconducting NiO Thin Films Deposited by Sol–Gel Technique, J. Chem. Mater. Res. 5 (2016) 119–122.
40. Schmachtenberg V.A.V., Tontini G., Koch J.A., Semione G.D.L., Drago V., Low temperature solventless syntheses of nanocrystalline nickel sulfides with different sulfur sources, J. Phys. Chem. Solids 87 (2015) 253–258.
41. Reddy A.J., Kokila M.K., Nagabhushana H., Sharma S.C., Rao J.L., Shivakumara C., Nagabhushana B.M., R.P.S. Chakradhar, Structural, EPR, photo and thermoluminescence properties of ZnO:Fe nanoparticles, Mater. Chem. Phys. 133 (2012) 876-883.
42. Boughalmi R., Boukhachem A., Kahlaoui M., Maghraoui H., Amlouk M., Physical investigations on Sb2S3 sprayed thin film for optoelectronic applications, Mater. Sci. Semicon. Proc. 26 (2014) 593-602.
43. Caglar M., Ilican S., Caglar Y., Influence of dopant concentration on the optical properties of ZnO: in films by sol–gel method, Thin Solid Films 517 (2009) 5023-5028.
44. J. Tauc, A. Menth, States in the gap, J. Non-Cryst. Solids 8-10 (1972) 569-585.
45. Slama S., Bouhafs M., Ben Mahmoud K.B., Boubaker A, polynomials solution to heat equation for monitoring A3 point evolution during resistance spot welding, I. J. Heat Techn. 26 (2008) 141-149.
46. Pankove J.I., in: Optical Processes in Semiconductors, Prentice-Hall, New Jersey, 1971, p. 92